JCI The Journal of Clinical Investigation

Pharmacologic targeting of a stem/progenitor population in vivo is associated with enhanced bone regeneration in mice

Siddhartha Mukherjee, … , Kenneth C. Anderson, David T. Scadden

J Clin Invest. 2008;118(2):491-504. https://doi.org/10.1172/JCI33102.

Research Article

Drug targeting of adult stem cells has been proposed as a strategy for regenerative medicine, but very few drugs are known to target stem cell populations in vivo. Mesenchymal stem/progenitor cells (MSCs) are a multipotent population of cells that can differentiate into muscle, bone, fat, and other cell types in context-specific manners. Bortezomib (Bzb) is a clinically available proteasome inhibitor used in the treatment of multiple myeloma. Here, we show that Bzb induces MSCs to preferentially undergo osteoblastic differentiation, in part by modulation of the bone-specifying transcription factor runt-related transcription factor 2 (Runx-2) in mice. Mice implanted with MSCs showed increased ectopic ossicle and bone formation when recipients received low doses of Bzb. Furthermore, this treatment increased bone formation and rescued bone loss in a mouse model of osteoporosis. Thus, we show that a tissue-resident adult stem cell population in vivo can be pharmacologically modified to promote a regenerative function in adult animals.

Pharmacologic targeting of a stem/progenitor population in vivo is associated with enhanced bone regeneration in mice

Siddhartha Mukherjee,[1,2,3,4] Noopur Raje,[3,5] Jesse A. Schoonmaker,[1,4] Julie C. Liu,[6] Teru Hideshima,[5] Marc N. Wein,[7] Dallas C. Jones,[7] Sonia Vallet,[5] Mary L. Bouxsein,[8] Samantha Pozzi,[5] Shweta Chhetri,[5] Y. David Seo,[1,4] Joshua P. Aronson,[1,4] Chirayu Patel,[4] Mariateresa Fulciniti,[5] Louise E. Purton,[1,4] Laurie H. Glimcher,[7] Jane B. Lian,[6] Gary Stein,[6] Kenneth C. Anderson,[5] and David T. Scadden[1,2,3,4]

[1]Center for Regenerative Medicine, Massachusetts General Hospital and Harvard Medical School, Boston, Massachusetts, USA. [2]Harvard Stem Cell Institute, Harvard University, Cambridge, Massachusetts, USA. [3]Massachusetts General Hospital Cancer Center, Boston, Massachusetts, USA. [4]Department of Stem Cell and Regenerative Biology, Harvard University, Cambridge, Massachusetts, USA. [5]Jerome Lipper Multiple Myeloma Center, Dana Farber Cancer Institute, Harvard Medical School, Boston, Massachusetts, USA. [6]Department of Cell Biology, University of Massachusetts, Worcester, Massachusetts, USA. [7]Department of Immunology and Infectious Diseases, Harvard School of Public Health, Boston, Massachusetts, USA. [8]Department of Orthopaedic Surgery, Beth Israel Deaconess Medical Center and Harvard Medical School, Boston, Massachusetts, USA.

Drug targeting of adult stem cells has been proposed as a strategy for regenerative medicine, but very few drugs are known to target stem cell populations in vivo. Mesenchymal stem/progenitor cells (MSCs) are a multipotent population of cells that can differentiate into muscle, bone, fat, and other cell types in context-specific manners. Bortezomib (Bzb) is a clinically available proteasome inhibitor used in the treatment of multiple myeloma. Here, we show that Bzb induces MSCs to preferentially undergo osteoblastic differentiation, in part by modulation of the bone-specifying transcription factor runt-related transcription factor 2 (Runx-2) in mice. Mice implanted with MSCs showed increased ectopic ossicle and bone formation when recipients received low doses of Bzb. Furthermore, this treatment increased bone formation and rescued bone loss in a mouse model of osteoporosis. Thus, we show that a tissue-resident adult stem cell population in vivo can be pharmacologically modified to promote a regenerative function in adult animals.

Introduction

Multipotent bone marrow stromal cells capable of giving rise to osteoblasts, adipocytes, and chondrocytes (a population termed mesenchymal stem/progenitor cells [MSCs]) were originally described by Friedenstein in 1966 (1, 2). Since that time, many groups have tried to examine these cells as therapeutic platforms in humans for orthopedic, cardiac, and immunologic conditions (3–5) using transplantation-based strategies, but the capacity to target endogenous MSCs toward particular lines of differentiation in vivo using pharmacological agents has remained relatively unexploited as a potential means for tissue regeneration. In general, small molecules that can therapeutically influence tissue-resident progenitor or stem cells in vivo have rarely been defined (6).

Pharmacologic targeting of stem/progenitor cells is an attractive concept but can only be achieved if candidate stem cell populations and modifying drugs with minimal toxicities can be identified. We sought to determine whether bortezomib (Bzb) might influence MSCs based on the incidental clinical observation that multiple myeloma patients treated with the drug were noted to have an increase in serum levels of bone-specific alkaline phosphatase (6–8). Others had previously noted that proteasome inhibitors could increase osteoblast number, function, and gene expression, although the specific target cell had yet to be identified and drugs could often not be administered therapeutically due to limited bioavailability or toxicity (9–11). A recent investigation also revealed that osteoblastic differentiation of human preosteoblasts could be increased by proteasome inhibition in vitro, raising the possibility that the same strategy could be used in a regenerative setting in vivo (11).

In this study, we show that the treatment of mice with low doses of Bzb (approximately one-fifth to one-third the dose equivalent required for antitumor effect) increased osteoblastogenesis, bone formation, and mineralized trabecular bone. By fractionating subpopulations of cells, we show that a relatively primitive population of stromal cells, but not their differentiated progeny, responds to Bzb. These studies raise the possibility that drug-induced progenitor/stem cell differentiation could be used in vivo to therapeutically modulate bone formation from a primitive reservoir of cells and that an existing clinical-grade drug can be "repurposed" to modulate stem biology. This strategy may be applicable to increase bone volume in the osteolytic disease of malignancy or in osteoporosis, where the function of more mature populations of cells has been compromised.

Results

Bzb increases serum osteocalcin, trabecular bone, osteoblast number, and bone marrow–derived osteogenic CFUs in mice. To determine the effect of Bzb on murine osteogenesis, mice were treated with the drug at

Nonstandard abbreviations used: Alp, alkaline phosphatase; API, alkaline phosphatase index; BFR, bone formation rate; BMD, bone mineral density; BMP-2, bone morphogenetic protein–2; BSP, bone sialoprotein; BSpm, bone surface perimeter; Bzb, bortezomib; hMSC, human MSC; MSC, mesenchymal stem/progenitor cell; MSGM, MSC growth medium; Op, osteoprogenitor; Osx, osterix; qPCR, quantitative PCR; Runx-2, runt-related transcription factor 2; Shn3, Schnurri-3; TRAP, tartrate-resistant acid phosphatase.

Conflict of interest: David Scadden serves as a consultant to and owns stock in Fate Therapeutics, Seattle, Washington, USA.

Citation for this article: *J. Clin. Invest.* **118**:491–504 (2008). doi:10.1172/JCI33102.

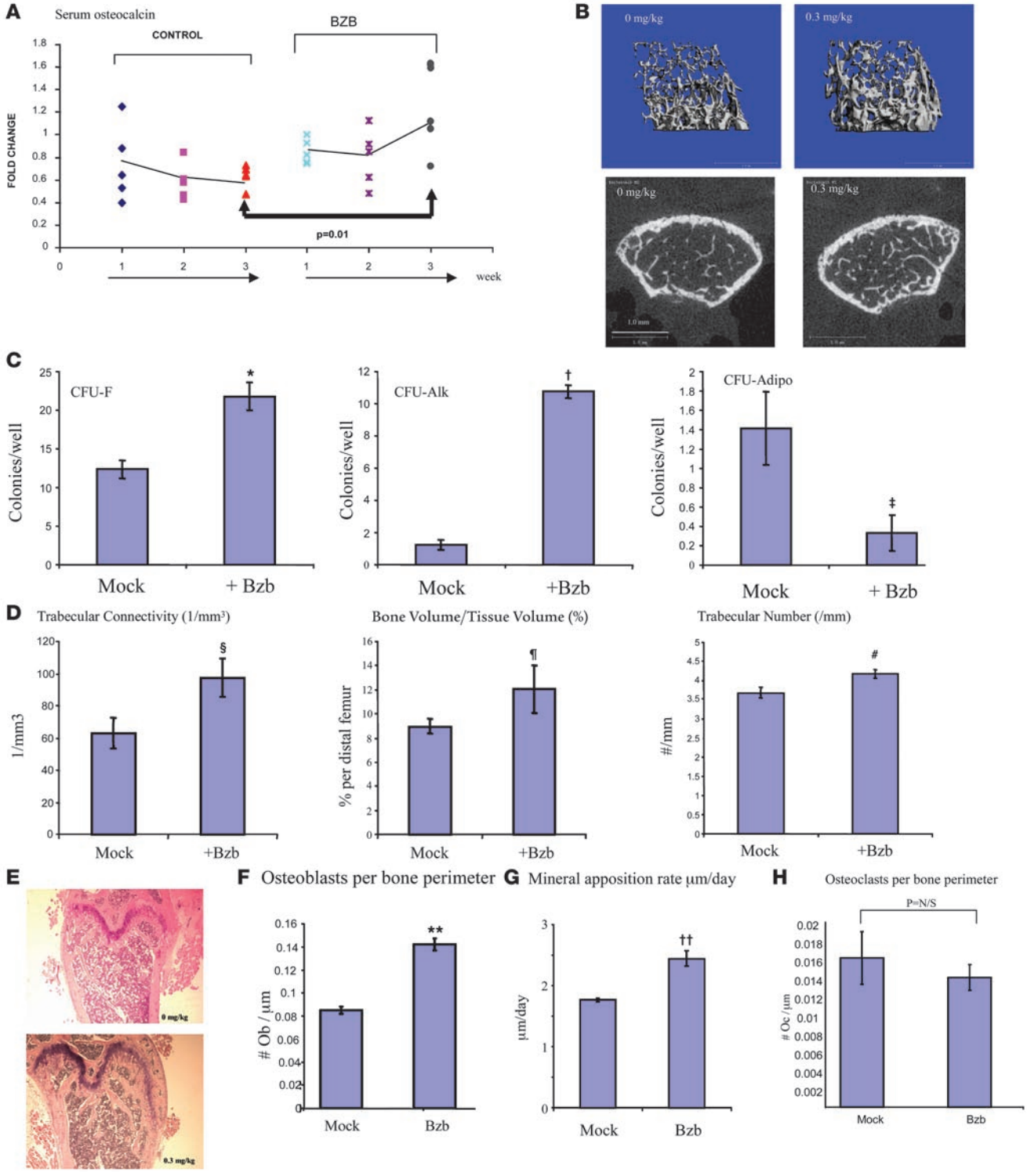
A
Serum osteocalcin
CONTROL
BZB
FOLD CHANGE
p=0.01
week
B
0 mg/kg
0.3 mg/kg
0 mg/kg
0.3 mg/kg
C
CFU-F
Colonies/well
Mock
+ Bzb
CFU-Alk
Colonies/well
Mock
+Bzb
CFU-Adipo
Colonies/well
Mock
+ Bzb
D
Trabecular Connectivity (1/mm³)
1/mm3
Mock
+Bzb
Bone Volume/Tissue Volume (%)
% per distal femur
Mock
+Bzb
Trabecular Number (/mm)
#/mm
Mock
+Bzb
E
0 mg/kg
0.3 mg/kg
F Osteoblasts per bone perimeter
Ob / µm
Mock
Bzb
G Mineral apposition rate µm/day
µm/day
Mock
Bzb
H
Osteoclasts per bone perimeter
P=N/S
# Oc / µm
Mock
Bzb

Figure 1
Bzb treatment increases osteoblasts in vivo. (**A**) Mice treated with Bzb (0.3 mg/kg i.p.; 3 times/week) showed an increase in the levels of serum osteocalcin over 3 weeks compared with control-treated (saline-treated) mice. In contrast, serum osteocalcin decreased over time in control mice. $P = 0.01$ by Student's t test; $n = 5$ mice each. (**B**) Micro-CT analysis revealed an increase in trabecular bone volume in drug-treated mice. A representative reconstruction of trabecular bone is shown as 3D reconstruction (left panel, mock treated; right panel, Bzb treated) and as cross sections (left panel, control; right panel, Bzb treated). Scale bar: 1.0 mm. (**C**) Colony formation from Bzb-treated versus saline-treated (mock-treated) animals showed increased CFU-F, increased Ops (CFU-Alk), and decreased adipocytic colonies (CFU-Adipo). $^{*}P = 0.007$, $n = 8$ wells for CFU-F; $^{\dagger}P < 0.01$, $n = 9$ wells for CFU-Alk; $^{\ddagger}P = 0.01$, $n = 12$ wells for CFU-Adipo. (**D**) Histomorphometric analysis of Bzb-treated animals showed increased trabecular connectivity, trabecular volume occupied by bone, and trabecular number. $^{\S}P = 0.05$, trabecular connectivity; $^{\P}P = 0.02$, trabecular bone volume; $^{\#}P = 0.03$, trabecular number/mm. $n = 4$ femurs. (**E**) Histological sections of treated animals showed increased bone with normal architecture in trabeculae (H&E-stained samples) but with increased bone volume. Original magnification, ×40. (**F**) Increased osteoblast number per BSpm in distal femur was observed in Bzb-treated animals. $^{**}P = 0.02$; $n = 3$. (**G**) Increase in mineralization rate in animals treated with Bzb. $^{\dagger\dagger}P < 0.01$; $n = 6$. (**H**) No significant change was observed in TRAP-stained osteoclasts, quantified by osteoclasts/μm of BSpm. $P = 0.53$ by Student's t test.

varying doses and serum osteocalcin, a surrogate marker for bone formation activity, was measured in vivo. At a dose of 0.3 mg/kg (doses typically used for antitumor effect in mice are 0.6–1.3 mg/kg), treatment for 3 weeks resulted in a significant increase in serum osteocalcin compared with vehicle-treated mice (Figure 1A) (the effect was also seen at 0.05 and 0.l mg/kg; data not shown). After 3 weeks of treatment, femurs were analyzed by quantitative micro-CT scanning. Trabecular volume, trabecular number, and trabecular density (Figure 1, B, D, and E) in the distal femur were all increased in drug-treated animals. Histomorphometric analysis on plastic sections revealed an increase in osteoblast number (Figure 1F) and mineral apposition rate (Figure 1G). Tartrate-resistant acid phosphatase (TRAP) staining revealed no significant change in osteoclasts per bone surface perimeter (BSpm, defined as total bone surface length per tissue section) in the secondary spongiosa (Figure 1H).

To determine whether the effect of Bzb was occurring at a stem/progenitor cell level, we performed several in vitro and in vivo studies. MSC activity is typically assessed by the ability of these cells to form stromal colonies (CFU-F) in vitro. In Bzb-treated animals, CFU-F was increased. When the differentiation potential of stromal cells was assessed by plating out CFUs in osteogenic and adipogenic conditions, there was a skewing of colonies toward osteogenic lineage (measured as alkaline phosphatase–positive CFU-Alk) versus adipogenic cells (CFU-Adipo) (Figure 1C). Bzb treatment in vitro (i.e., *after* the plating of untreated primary cells) had no effect on the CFU-Alk (data not shown). Although alternative hypotheses may explain these findings, these results suggested that Bzb treatment of animals targets a marrow-resident cell population that possesses the capacity for bilineage differentiation and the ability to form MSC stromal colonies in vitro.

Bzb promotes osteoblastogenesis in purified murine MSCs. Murine bone marrow MSCs can be obtained by culturing plastic adherent bone marrow stromal cells in vitro; these cells have the ability to be serially passaged, retain multipotency, and have been antigenically characterized as $CD105^{+}$, $CD45^{-}$, and hematopoietic lineage negative (12–15). To determine whether MSCs respond to Bzb in vitro, plastic-adherent MSC stromal cultures were established from a mouse expressing GFP under the control of an actin promoter (GFP expression was used as a marker in subsequent transplant studies). At 3 to 4 weeks after the establishment of these cultures (i.e., at passages 2–4), $CD105^{+}$ cells were positively selected using magnetized biotinylated beads (the cells were also $CD45^{-}$ and lineage negative by FACS analysis and represented between 2% and 5% of the original cultures). Under osteogenic conditions, exposure of this cell population to Bzb increased the number of alkaline phosphatase–positive cells (Figure 2B). To further characterize the response of this cell population to Bzb, we measured the transcription of 2 genes: bone sialoprotein (*BSP*), a marker of differentiated osteoblasts, and *Runx-2*, which is obligate for osteogenesis. In purified $CD105^{+}$ cells, Bzb treatment significantly increased the expression of *BSP* and *Runx-2* as detected by quantitative PCR (qPCR) analysis (Figure 2C). In contrast, when the same cells were predifferentiated into presumptive osteoblasts using osteogenic medium for 7 days (a point of time when *BSP* expression increases nearly 80-fold and mineralized nodules begin to appear in vitro), they lost the responsiveness to Bzb. Bzb treatment of MSCs also increased von Kossa staining in in vitro cultures (a measure of calcified extracellular matrix formation), while predifferentiated cells showed no increase in staining (Figure 2D). When MSCs were subjected to adipogenic differentiation in the presence of Bzb, a decreased number of oil red O staining cells was observed, suggesting that osteogenesis and adipogenesis were being reciprocally affected by Bzb.

In contrast to MSCs, osteoprogenitors (Ops) and osteoclasts also did not respond to Bzb treatment. To investigate the effect of Bzb on Ops, we used a mouse strain in which Ops are marked by the expression of a GFP-Cre fusion protein under the control of the osterix (*Osx*) promoter (16, 17). *Osx* is expressed during early osteogenic commitment (after *Runx-2* expression) and downregulated as cells progress into mature osteoblasts (17). We isolated $CD45^{-}GFP^{+}$ cells from Osx-GFP compact bone to obtain a population of GFP^{+} Op-rich fraction (10,000 cells/mouse) and a GFP^{-} Op-depleted fraction. The Op-enriched fraction did not show a response to Bzb as measured by collagen I staining while the Op-depleted ($CD45^{-}GFP^{-}$) fraction, containing the undifferentiated (i.e., uncommitted) MSCs, showed a response (Figure 3). We do note, however, that Osx-positive Ops, which are downstream of *Runx-2* activation (17), appear to have a relatively poor proliferative capacity in vitro compared with the highly proliferative MSCs. Since osteogenesis depends on the proliferation and density of cells, the absence of responsiveness may thus reflect a general ability of this subpopulation of cells to form appropriately dense colonies in vitro.

Osteoclasts were also insensitive to Bzb at these doses in vitro. Osteoclasts were derived from bone marrow cells in the presence of M-CSF and RANKL. TGF-β served as a positive control and caused a significant increase in TRAP activity, while the addition of Bzb did not affect TRAP activity of these cultures (Supplemental Figure 1A; supplemental material available online with this article; doi:10.1172/JCI33102DS1). Bzb also had no effect on the size of pits formed by osteoclasts in vitro, suggesting that the resorptive activity of osteoclasts was unaffected at these doses (Supplemental Figure 1B).

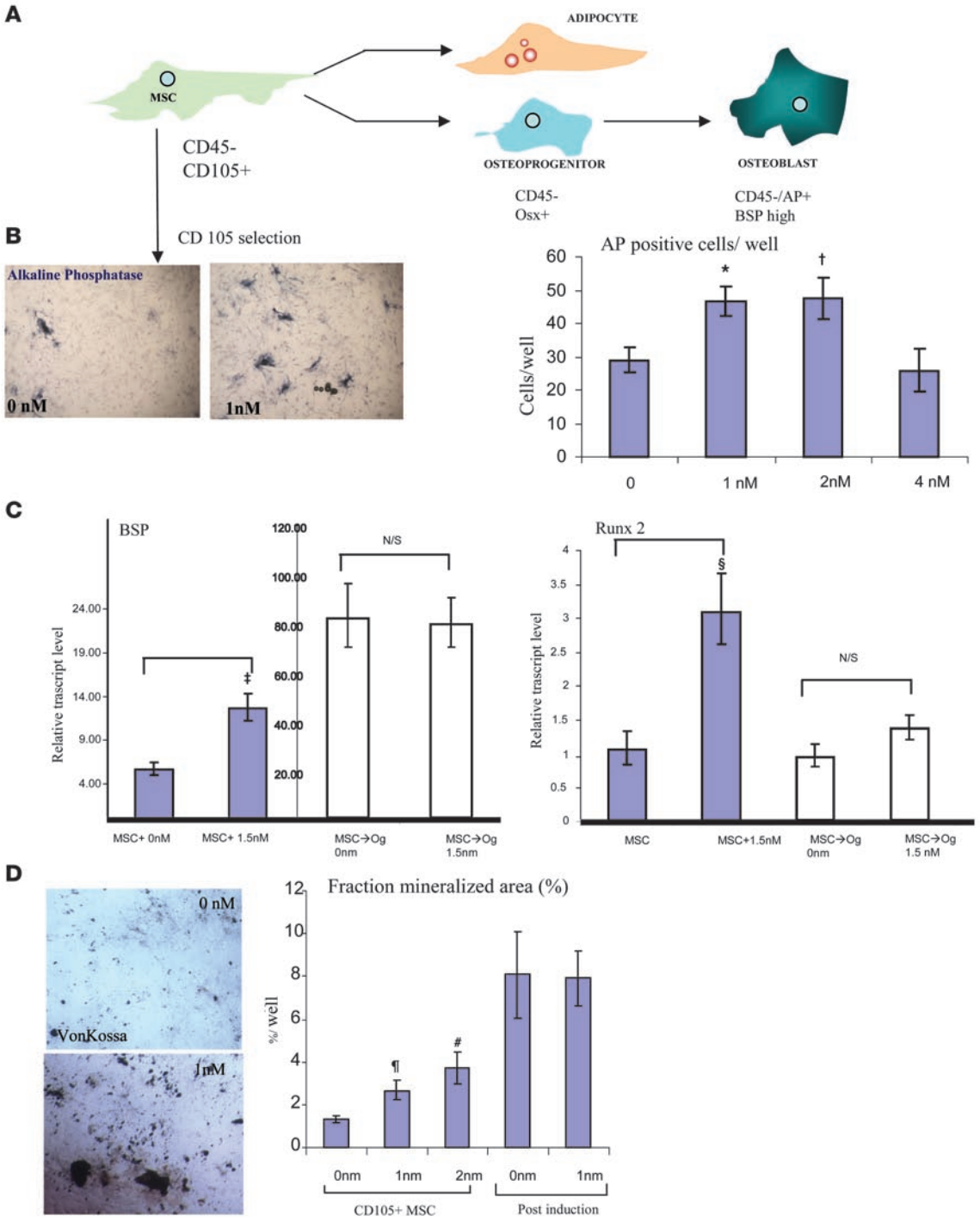

Figure 2

Bzb increases osteoblastogenesis in MSCs in vitro. (**A**) Murine MSCs are multilineage-potent fibroblastoid cells that can differentiate into osteoblasts and adipocytes; they are hematopoietic lineage negative, CD45$^-$, and CD105$^+$. Ops are Osx positive. Upon differentiation, MSCs lose 105 staining, form von Kossa staining ECM nodules, and express high levels of BSP. (**B**) Isolated murine MSCs (CD105-selected cells) showed increased alkaline phosphatase activity, blue staining (left panel, control; right panel, 1 nM). Alkaline phosphatase–positive cells per well increased with 1 and 2 nM of Bzb. *P = 0.01; †P = 0.01; n = 6 wells each. Original magnification, ×100. (**C**) CD105-selected cells exposed to osteogenic medium with or without 1.5 nM Bzb were analyzed by qPCR. BSP transcript levels and Runx-2 transcript levels (plotted against the baseline value of untreated MSCs assigned as 1.00) increased significantly in Bzb-treated samples at 30 hours (‡P = 0.04; §P = 0.03; n = 2), while preexposure to osteogenic differentiation (MSC→Og) for 8 days followed by Bzb treatment abrogated the response (white bars for 0 and 1.5 nM; P = NS). (**D**) Von Kossa–positive area increased with 1 and 2 nM Bzb. ¶P = 0.05; #P = 0.01; n = 3 wells. Original magnification, ×100.

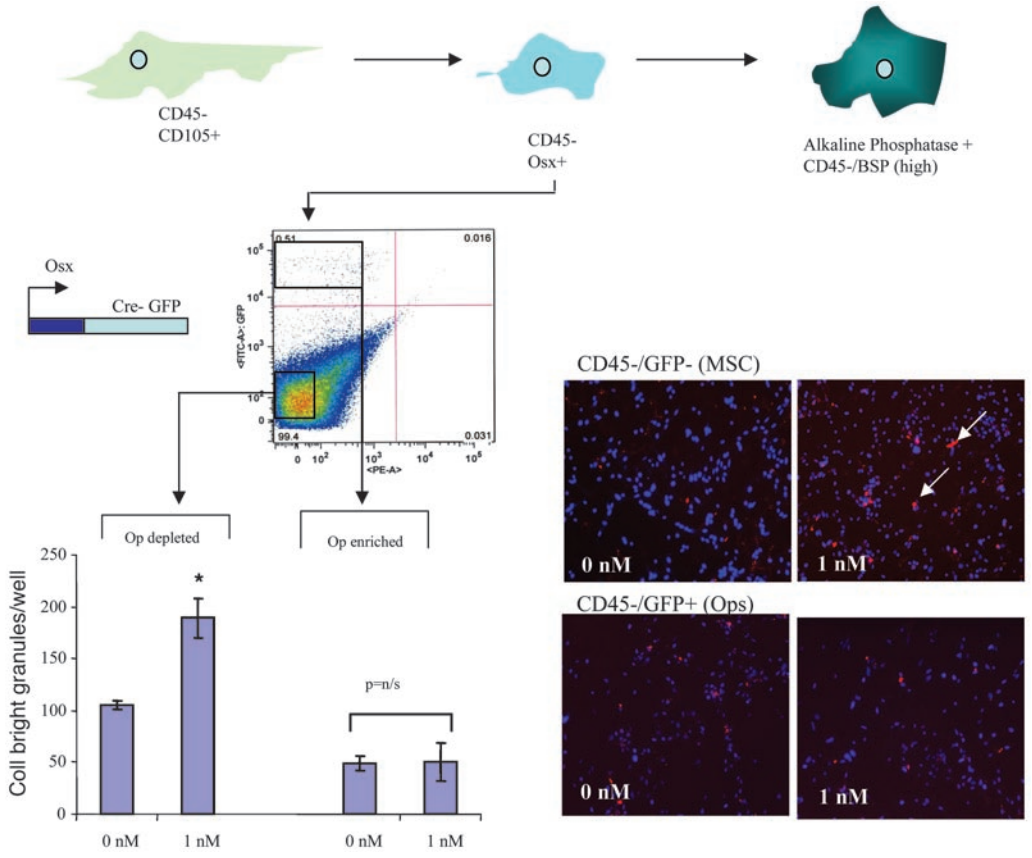

Figure 3
Osx-positive Op cells do not respond to Bzb, while Osx-negative MSCs respond to Bzb in vitro. Ops were recovered from the compact bone of *Osx-GFP* mice by isolation of $CD45^{-}GFP^{+}$ cells. $CD45^{-}GFP^{+}$ Ops plated in vitro showed no change in collagen I clusters, while $CD45^{-}GFP^{-}$ MSCs isolated from the same mice showed an increase (arrows). $^{*}P < 0.05$; $n = 4$. Original magnification, ×100.

We next determined whether the effects of Bzb on murine MSCs could be recapitulated in human bone marrow MSCs. These cells have been extensively characterized by other groups and are available for research use as a standardized reagent (18–21). By immunophenotype, these cells were homogenously $CD105^{+}CD73^{+}CD11b^{-}CD31^{-}CD45^{-}$ and were capable of multilineage differentiation (data not shown). When primary human MSCs (hMSCs) were exposed to Bzb, there was an increase in alkaline phosphatase index (API) (Figure 4A) and in alizarin red staining (Figure 4B) and a decrease in adipocytes (Figure 4C). These data suggest that hMSCs and mouse MSCs respond comparably to Bzb.

Bzb stabilizes Runx-2 degradation and depends on the presence of Runx-2 to increase osteoblastogenic genes. Next, we investigated a potential mechanism for the effect of Bzb on osteoblastic differentiation. The transcription factor *Runx-2* (*CBFA-1*) is known to be the earliest expressed of the essential regulators of osteogenic differentiation (22, 23). Runx-2 is degraded by the proteasome and reciprocally affects osteogenic versus adipogenic differentiation (24–26). To investigate whether Bzb affects Runx-2 degradation, MSC cultures were treated with Bzb in vitro under baseline, nonosteogenic conditions (in the absence of dexamethasone, ascorbate, and β-glycerol phosphate) for 6 hours. Bzb increased the steady-state levels of Runx-2, particularly of the p62 isoform, associated with osteogenic commitment (26). Treatment with lactacystin (Figure 5A), a structurally unrelated proteasome inhibitor, demonstrated a similar effect on Runx-2 protein stability (Figure 5A). The transcriptional level of *Runx-2* under these conditions was unaffected by Bzb treatment as measured by qPCR (data not shown). Runx-2 is also known to be a potent activator of the osteocalcin gene (26, 27), and we next asked whether Bzb-mediated Runx-2 stabilization might increase the expression of a *Runx-2* target gene. To test this, we used a reporter system consisting of a vector that expresses firefly luciferase under the control of 6 Runx-2 binding elements derived from the osteocalcin gene (27). When a *Runx-2*–expressing vector was cotransfected with this reporter construct into C3HT1/2 fibroblasts (that have negligible endogenous Runx-2 activity), an increase in luciferase activity was noted. Notably, treatment with both Bzb and the proteasome inhibitor lactacystin led to a significant further increase in luciferase activity, suggesting that proteasome inhibitor–mediated Runx-2 stabilization can increase the transcriptional activity of *Runx-2* (Figure 5B).

Normally, Runx-2 is recruited for ubiquitination and subsequent proteasomal destruction by the adaptor protein Schnurri-3 (Shn3) (27). In $Shn3^{-/-}$ MSCs, Runx-2 levels are endogenously high (Figure 5A), leading to increased osteogenesis in vivo. If Bzb is acting through the Runx-2 pathway, then endogenous upregulation of Runx-2, resulting in accelerated differentiation of mature osteoblasts, should abrogate the responsiveness of MSCs to the drug. To test this hypothesis, we treated WT and $Shn3^{-/-}$ MSCs with Bzb. In WT cells, Bzb treatment led to an increase in von Kossa–positive bone nodules (Figure 5C). In contrast, von Kossa–staining ECM nodules in $Shn3^{-/-}$ cells were markedly elevated at baseline but remained unchanged with Bzb treatment.

Conversely, deletion of *Runx-2* may be expected to decrease osteogenic differentiation and the responsiveness to Bzb. $Runx\text{-}2^{-/-}$ MSCs could not be obtained because $Runx\text{-}2^{-/-}$ mice are unable to form mineralized bone and die in utero (22, 23, 27, 28). However, embryonic mesodermal fibroblasts can be derived from these mice.

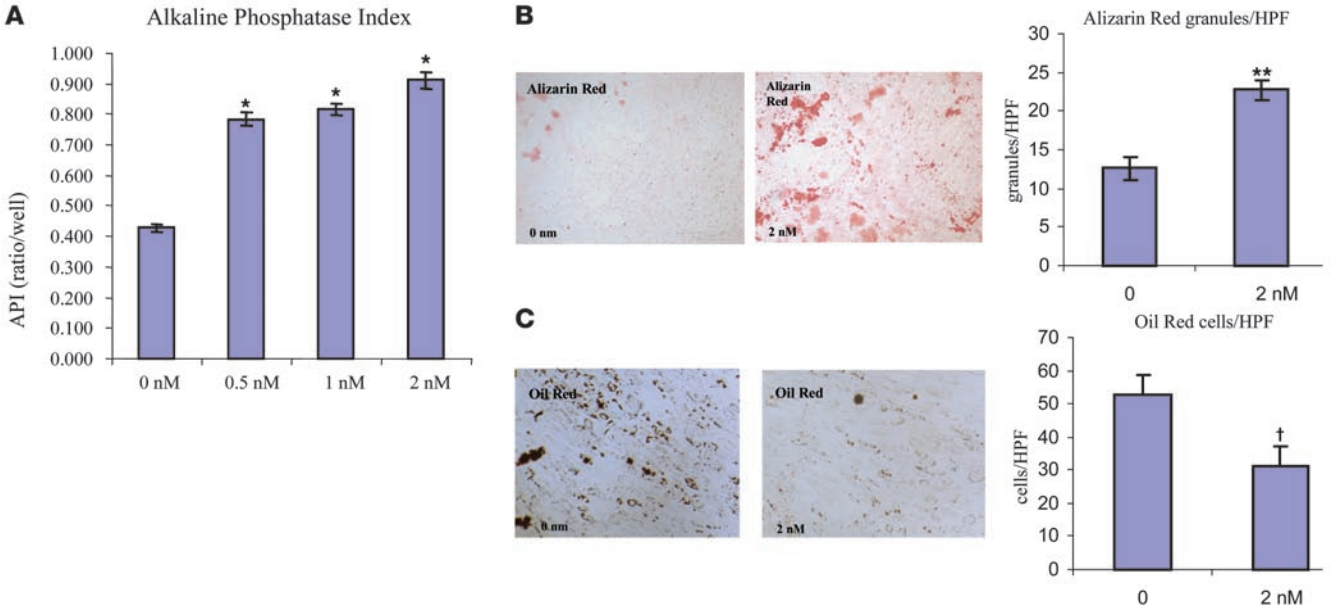

Figure 4
Bzb acts on hMSCs. (**A**) hMSCs ($CD105^+CD73^+CD45^-$) were subjected to Bzb in vitro, and API was assessed after 6 days in culture. API measurements revealed an increase in activity with 0.5, 1, and 2 nM Bzb. $^*P = 0.001$; $n = 10$. (**B**) Alizarin red staining was increased upon Bzb treatment. $^{**}P = 0.002$; $n = 5$ fields. (**C**) Adipocytes (oil red O–positive cells) were decreased. Original magnification, ×100. $^\dagger P = 0.03$; $n = 4$ fields.

The WT cells express Runx-2 and can differentiate into adipocytes and osteoblasts capable of giving rise to mineralized nodules in vitro (29). Embryonic mesodermal fibroblasts from *Runx-2*$^{-/-}$ mice (versus WT controls) were treated with Bzb in vitro and assessed for osteogenic differentiation using a panel of 3 genes. For 2 genes (*BSP* and alkaline phosphatase [*Alp*]), *Runx-2*$^{-/-}$ cells did not show responsiveness to Bzb compared with WT cells (Figure 5D). For the third gene, collagen I, both WT and Runx-2$^{-/-}$ cells showed increased expression with Bzb treatment. Exposure to bone morphogenetic protein–2 (BMP-2), a bone-inducing signaling molecule, accelerated the conversion of the WT (i.e., *Runx-2* intact) cells into Ops (reflected by the upregulation of osteogenic genes such as *osteocalcin* and *BSP*) and rendered them unresponsive to Bzb. These results suggest that although some genes involved in osteoblastogenesis, such as collagen I, may be increased by Bzb even in the absence of *Runx-2*, Bzb depends on the presence of *Runx-2* to increase the expression of other genes obligate for osteoblastogenesis. Thus, *Runx-2*–dependent osteogenesis is a pathway critical to the Bzb response. However, Bzb must also target other pathways in MSCs, since the effect of Bzb on collagen I was still maintained despite *Runx-2* ablation.

Implanted hMSCs and mouse MSCs respond to Bzb in vivo. We next sought to determine whether MSCs respond to Bzb in vivo. MSCs can be implanted into mice, and they engraft and differentiate and can thus be assessed in vivo (30, 31). We performed 2 studies. First, undifferentiated hMSCs or MSCs preinduced to osteoblastic differentiation for 1 week were loaded into collagen sponges and implanted subcutaneously in immunodeficient mice. Under these conditions, MSCs typically form ectopic bone while osteoblasts show limited mineralization capability (this model has been extensively used to determine the differentiation activity of MSCs) (30). After implantation, animals were treated either with Bzb or saline for 10 doses (3 times a week for 27 days). In MSC-loaded sponges, Bzb treatment enhanced the formation of ectopic bone (Figure 6A) and increased the presence of mineralizing osteoblasts, assessed by endosteal cells associated with the matrix-incorporated dye xylenol orange (Figure 6A). Sponges containing cells that had already been exposed to osteogenic differentiation medium in vitro (i.e., before implantation) showed no response to Bzb. Undecalcified sponges containing MSCs were sectioned and stained with alizarin red (Figure 6A) to stain calcified matrix, and the fraction of tissue staining positive for alizarin was found to be significantly increased for Bzb-treated mice.

Second, we implanted GFP^+ murine MSCs into the bones of sublethally irradiated mice by direct intrafemoral injection (31). The mice were then treated with Bzb or saline. MSCs and MSC-derived cells were identified by GFP expression (Figure 6B), and osteoblasts were marked by alkaline phosphatase staining. In saline-treated animals, GFP^+ MSCs gave rise to some ectopic mineralization. A few GFP^+ osteoblasts were observed occupying their normal positions at the endosteal surface, but most GFP^+ donor cells remained alkaline phosphatase negative (Figure 6B). In contrast, in Bzb-treated mice, abundant ectopic mineralization was observed in the intrafemoral space. Notably, donor-derived ectopic osteoblasts (alkaline phosphatase–positive, GFP-positive cells) appeared several cell layers beyond the endosteal surface (Figure 6B). In saline-treated mice, implanted MSCs typically retained the expression of the MSC marker CD105, while in Bzb-treated animals, GFP^+ cells were typically found embedded inside mineral and had lost CD105 expression (Figure 6B). Taken together, these results suggest that, in this transplantation system, bone regeneration is induced from implanted MSCs upon treatment with Bzb.

Bzb increases trabecular bone volume and bone formation in ovariectomized mice. To determine whether drug-induced MSC differentiation might rescue bone loss in a disease state, ovariectomized adult 9-week-old female mice were treated with saline or with Bzb

2.5 weeks after ovariectomy. Nonovariectomized mice treated with Bzb showed the previously observed increase in bone mineral density (BMD), trabecular bone volume compared with saline-treated controls. As expected, ovariectomized mice experienced a decrease in BMD and trabecular volume. However, treatment with Bzb for 6 weeks (18 doses) partially rescued the osteoporotic phenotype: BMD, trabecular number, and trabecular density increased, and the mineralized architecture appeared similar to normal bone (Figure 7, A and B), demonstrating that Bzb-induced MSC differentiation may be therapeutically useful in this mouse model of tissue degeneration. Dynamic histomorphometry was performed to evaluate bone formation under these conditions. In sham-treated (i.e., nonovariectomized) mice, Bzb treatment caused an increase in bone formation rate (BFR) as previously observed. In ovariectomized mice, there was also a relative increase in BFR above baseline (consistent with prior studies that suggest increased osteoblast activity in the face of estrogen depletion; ref. 32). Notably, Bzb treatment further increased the BFR (per unit BSpm) in ovariectomized mice (Figure 7C). Similar trends were observed in mineral apposition rates, but the increase in mineral apposition in ovariectomized mice with Bzb was not statistically significant. Thus, Bzb increases bone formation and trabecular bone volume in the setting of osteoporosis.

Discussion

Our data show that Bzb, a first-in-class proteasome inhibitor available for human use, can enhance the differentiation of MSCs toward osteoblasts. Although proteasome inhibition may have diverse pleiotropic effects in humans, surprisingly few populations of normal (i.e., nonmalignant) cells have emerged as targets of Bzb treatment thus far. It is likely that other cellular targets may emerge, but the limited adverse effects profile of a drug with such a ubiquitously expressed molecular target (Supplemental Figure 2) is remarkable and bears commentary. Either Bzb has specificity for only certain cell types (by virtue of differences in proteasomal composition in different cells) and/or only certain critical pathways in adult humans are sensitive to the particular changes in proteasomal function targeted by Bzb. We note that several key osteoblast differentiation factors — including *Gli-3* (identified in a prior study by Garrett et al.; ref. 10) and *Runx-2* — appear to be particularly sensitive to proteolytic processing and are thus targeted by proteasome inhibitors. By modulating the levels of these transcription factors, Bzb appears to be accelerating osteogenesis. Our data thus lend further support for the notion that small molecules of this class can have profound effects on bone formation at therapeutically achievable doses in humans.

One important limitation of this study is that the lineage tracking of endogenous MSCs is not possible since no single marker (or promoter) appears to define this population in vivo. However, direct transplantation of purified cells partially overcomes this limitation by virtue of markers (such as GFP) that enable us to track the fates of donor cells. This limitation is by no means restricted to MSCs. In the hematopoietic system, markers of endogenous hematopoietic stem or progenitor cells that efficiently enable the lineage tracking of these cells in situ are also unavailable. As such, any effect on "stem cells" or progenitors is typically evaluated by colony formation assays, purification of specific populations using lineage-specific markers followed by transplantation and functional outcomes. By analogy to the hematopoietic system, we thus used all 4 of these criteria to evaluate the effect of Bzb on MSCs. A second important limitation is that, while markers for murine and hMSCs (such as CD105) have been described, definitive markers for the positive selection of osteoblasts remain undefined. Thus, to identify the precise population of cells responsive to Bzb, improved lineage markers of mesenchymal differentiation are also needed but are presently unavailable. Finally, it is likely that aging plays an important role in the responsiveness of mesenchymal cells to osteoinductive stimuli, but this was not tested in the current study. Mice used for the study were typically 7 to 9 weeks old (and between 10 to 18 weeks at the end of the study period). At these points, bone mineralization in the C57BL/6 strain has already reached a peak value, but full skeletal maturity has not been achieved (33). Thus, whether Bzb might rescue the osteoporotic phenotype in aged mice remains an open question.

Despite these limitations, our findings have several implications for the biology and therapy of human diseases associated with tissue loss. Osteoporosis is a highly prevalent disease characterized by a progressive loss of mineralized bone. Many mechanisms contribute to this bone loss, but one important component is that osteoblastic activity is unable to compensate for bone loss induced by estrogen depletion. Uncompensated bone loss also occurs in malignant diseases when cancer cells migrate to the bone microenvironment, activate osteoclasts, and inhibit osteoblasts (34). Current therapies for these bone loss disorders have targeted mature cell populations (35) including osteoblasts and Ops (using pulsatile parathyroid hormone) and osteoclasts (using bisphosphonates), but these therapies have many intrinsic limitations. Long-term osteoclast inhibition also appears to inhibit osteoblast activity, and bisphosphonates have been recently implicated in osteonecrosis (36). Moreover, in osteolytic disease of malignancy, and in particular, in multiple myeloma (37–39), osteoblasts are decreased in number and activity, thus dampening the effect of any drug that targets osteoblasts.

The capacity to target the differentiation of more primitive populations of cells may therefore be attractive in settings where mature cell populations have been depleted or have become dysfunctional. In the case of osteoporosis, MSC implantation into fracture sites has been proposed as a regenerative strategy and is being evaluated clinically. Proteasome inhibition during the engraftment period may improve bone remodeling by inducing therapeutic differentiation of these cells. Although long-term treatment with Bzb may be unfeasible given its systemic toxicities, short-term treatment at lower doses may be a valuable means to augment bone formation. This strategy may also prove to be useful in the setting of osteolytic disease of malignancy, where factors elaborated by tumors activate osteoclasts and incapacitate or kill osteoblasts, thus severely dampening the effect of any drug that targets osteoblasts. Our results indicate that pharmacological manipulation of a progenitor cell population may be used in the context of tissue loss (in this case osteoporosis) to alter and improve tissue state during degeneration, an important goal for regenerative medicine.

Methods

In vivo treatment with Bzb. C57BL/6 mice (female, 7 weeks; Charles River Laboratories) were treated with 0, 0.05, 0.125, or 0.3 mg/kg of Bzb (or saline control) 3 times a week — Mondays, Wednesdays, and Fridays — by i.p. injection. Peripheral blood was collected weekly in the morning and osteocalcin levels assessed by ELISA (Biomedical Technologies Inc.) according to the manufacturer's instructions. Calcein double labeling was performed as previously described (40). For statistical analysis, values for serum osteo-

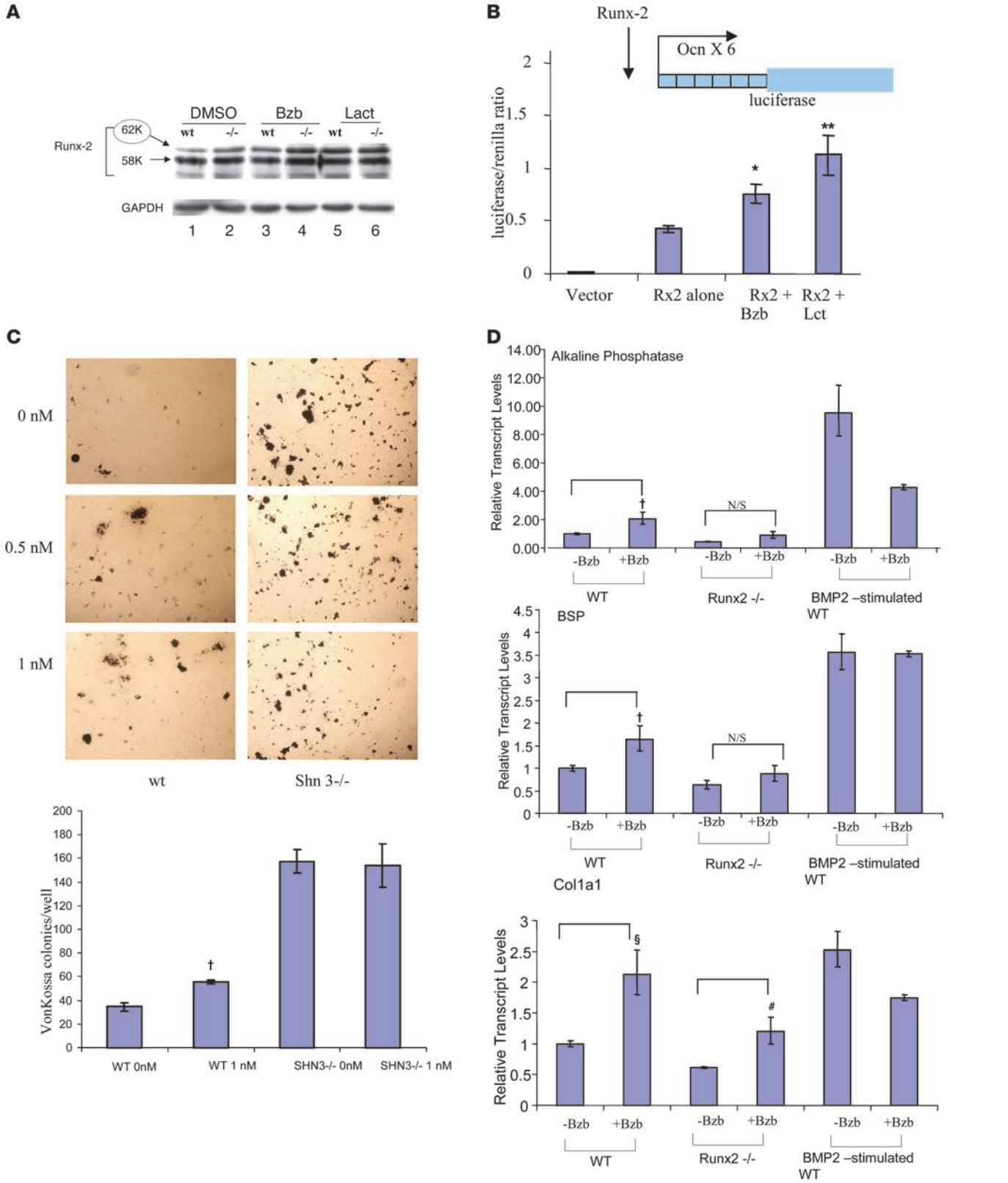
A
DMSO
Bzb
Lact
wt
-/-
62K
58K
Runx-2
GAPDH
1 2 3 4 5 6
B
Runx-2
Ocn X 6
luciferase
luciferase/renilla ratio
Vector
Rx2 alone
Rx2 + Bzb
Rx2 + Lct
C
0 nM
0.5 nM
1 nM
wt
Shn 3-/-
VonKossa colonies/well
WT 0nM
WT 1 nM
SHN3-/- 0nM
SHN3-/- 1 nM
D
Alkaline Phosphatase
Relative Transcript Levels
-Bzb
+Bzb
WT
Runx2 -/-
BMP2 –stimulated WT
N/S
BSP
Col1a1

Figure 5
Runx-2 modulates the responsiveness to Bzb. (**A**) Steady state levels of Runx-2 protein in MSCs from WT (lanes 1, 3, and 5) or *Shn3*$^{-/-}$ mice (lanes 2, 4, and 6) were detected by Western blotting of MSCs cultured either with DMSO vehicle, Bzb, or lactacystin. In WT MSCs, p62 Runx-2 (red circle) was upregulated by Bzb treatment (lane 1 versus lane 3) and by lactacystin (lane 1 versus lane 5) to levels comparable to Runx-2 levels in *Shn3*$^{-/-}$ MSCs (lane 2). Bzb and lactacystin also increased Runx-2 levels in Shn3$^{-/-}$ MSCs, suggesting that Shn3-independent proteasomal activity targeting Runx-2 still remains functional in these MSCs. Bottom panel shows *GAPDH* used as a loading control. (**B**) C3HT1/2 cells were transfected with a luciferase construct containing 6 Runx-2–binding elements from the osteocalcin gene. Cotransfection of a *Runx-2* expression construct (Rx-2) increased *luciferase* expression above baseline. Addition of either Bzb or lactacystin (third and fourth bars) further increased luciferase expression (*P = 0.0009; **P = 0.0003) compared with *Runx-2*–cotransfected cells without drug treatment. (**C**) MSCs from WT or Shn3$^{-/-}$ animals were plated in osteogenic medium. Von Kossa staining (brown) revealed a dose-dependent increase in osteogenic activity with Bzb treatment in WT mice, while in Shn3$^{-/-}$ mice, there was constitutively elevated von Kossa granule formation that was not increased by Bzb treatment. †P = 0.04; n = 4 wells. Original magnification, ×100. (**D**) In WT embryonic mesodermal fibroblasts (MEFs), treatment with Bzb showed an increase in expression of *Alp* and *BSP*, while in Runx-2$^{-/-}$ cells, there was no response (upper 2 panels); however, expression of collagen I (bottom panel) was increased in both WT (§P = 0.02) and *Runx-2*$^{-/-}$ cells (#P = 0.03). Stimulation of WT cells to promote Op formation with exogenous BMP-2 (two bars on far right of each panel) abolished the Bzb responsiveness of all 3 genes.

calcin at each point were normalized for every individual animal to its own osteocalcin level at week 0 (i.e., before treatment) and plotted as fold change. Differences in the groups were then analyzed by a 2-tailed Student's t test. Animal care, experiments, and protocols were approved by the Institutional Animal Care and Use Committee, Massachusetts General Hospital.

Colony formation assay. Spines from mice treated with saline or 0.3 mg/kg Bzb for 3 weeks (as above) were dissected and cleaned. A fixed mid-spine segment (approximately 4 cm) was crushed by mortar and pestle. After lysis of rbc, cells from 5 control and 5 treated mice were pooled and 1×10^6 primary bone marrow cells from each group (isolated as described below) were plated in 24-well plates in a medium composed of αMEM, 20% fetal bovine serum (HyClone), and penicillin and streptomycin solution (CellGro) — henceforth referred to as α20%. Medium was changed at 24 hours to eliminate nonadherent cells. For CFU-F assay, cells were left in α20%; for CFU-Alk, cells were moved to osteogenic medium (see below) on day 3; for CFU-Adipo, cells were left in α20% for 6 days to allow initial colony formation and then switched to adipogenic medium (see below). After 16 days, colonies were assessed by methylene blue staining for the CFU-F assay, BCIP staining (alkaline phosphatase) for CFU-Alk, or oil red O staining for CFU-Adipo (see below). Only colonies containing a majority of histologically stained cells (>50%) were scored as positive.

Histomorphometric analysis (static and dynamic). For histomorphometry, mice were treated with Bzb as above for the period specified. For experiments depicted in Figure 1, 7-week-old C57BL/6 female mice were used and treated for 3 weeks (9 doses). For experiments depicted in Figure 7, 9-week-old FVB/N female mice were either sham treated or ovariectomized and then housed for an additional 2.5 weeks (to allow for osteoporotic phenotype to develop) before starting Bzb treatment for 6 weeks. In both cases, at 10 days and 3 days before sacrifice, calcein was injected i.p. as previously described (40). Bones were fixed in 4% paraformaldehyde, and undecalcified sections embedded in plastic were sectioned at 8 μm. For static analysis depicted in Figure 1, sections were stained with toluidine blue. Images of the secondary spongiosa were obtained with a ×20 objective, and 2 images were obtained per section to cover the entire spongiosa. Osteoblasts were identified as mononuclear cells directly abutting either mineralized bone or osteoid and restricted within 1–3 cell diameters from the endosteal surface. For mineral apposition rates and BFRs, images of the secondary spongiosa were obtained as above, with simultaneous images in bright-field and under green fluorescence using a ×10 objective. Bright-field images were used to outline the BSpm, and then BSpm was calculated by ImageJ analysis (http://rsb.info.nih.gov/ij). Double-labeled areas (i.e., areas where both day –10 and day –3 calcein label was present) and single-labeled areas were also marked on the images. The average distance between double-labeled areas was calculated by ImageJ analysis using 3 measurements per double label. Mineral apposition rate (MAR) was calculated by dividing the average double-label distance (in μm) for each sample and dividing by the interlabel time of 7 days. To calculate BFR, the total length of double label and single label was calculated for each sample. BFR (with BSpm referent) was calculated as MAR × (0.5 single-label length + double-label length)/BSpm.

TRAP staining for osteoclasts. Femurs fixed in 4% paraformaldehyde were decalcified in EDTA and then sectioned after paraffin embedding. After deparaffinization, TRAP staining was carried out per manufacturer's protocol (387A-1KT; Sigma-Aldrich). Images of the secondary spongiosa were obtained as above, and the number of TRAP-positive cells abutting the endosteal surface was calculated for every section. BSpm was calculated by drawing lines manually on images and quantifying the length as above.

Isolation of primary bone marrow cells for MSCs. C57BL/6 actin-GFP mice (003291; Jackson Laboratories) were sacrificed; tibiae, femurs, and spine were removed and excess soft tissue was eliminated. Using a pestle and mortar, the bones were crushed and washed in PBS with 0.5% FBS and passed through a 70-μm filter into a collection tube. The slurry was spun at 470 *g* for 5 minutes; the supernatant was removed, and cells were resuspended in a minimal volume of ACK lysing buffer (Cambrex) for 4 minutes on ice and washed once with PBS. After pelleting once again, the cells were resuspended and plated in α20% and incubated at 33°C with 5% CO_2. After 4 weeks of culture and expansion, CD105 isolation was performed by magnetic isolation (Dynabeads M-280 Streptavidin; Invitrogen) or MACS beads (Miltenyi Biotech) using an anti-mouse CD105 biotin antibody (clone MJ7/18; eBioscience) at 10 μg/ml. The CD105-positive cells were then maintained in α20% as before. Passage number for experiments has been indicated below.

Alkaline phosphatase staining. Purified CD105$^+$ cells (passages 3–5) were isolated by MACS beads using a biotinylated CD105 antibody and plated at 2×10^3 cells/well in a 96-well plate (BD Biosciences) at 33° in osteogenic induction medium: α20% modified with glycerol 2-phosphate (2.16 mg/ml), 2-phospho-L-ascorbic acid (0.05 mg/ml), and dexamethasone (10 nM) (Sigma-Aldrich). After 18 hours of differentiation, alkaline phosphatase staining was carried out with BCIP/NBT solution (Sigma-Aldrich) per the manufacturer's instructions.

BSP and Runx-2 expression analysis. CD105$^+$ cells were isolated from MSC cultures as described above and plated at 5000/cm^2 in 6-well plates. On day 1 after plating, they were switched to osteogenic medium containing Bzb at 1.5 nM versus carrier (0 nm) alone. After 30 hours at 33°C, cells were immediately lysed into TRIZOL and were frozen for further analysis. In parallel experiments, the same cells were differentiated in osteogenic medium for 8 days and then switched into osteogenic medium containing 0 or 1.5 nM Bzb. At 30 hours, cells were again lysed into TRIZOL as described above. RNA isolation, qPCR, normalization, and statistical analysis were as described below for embryonic fibroblasts except that transcript levels were normalized to *GAPDH* (primers were from Applied Biosystems; see below).

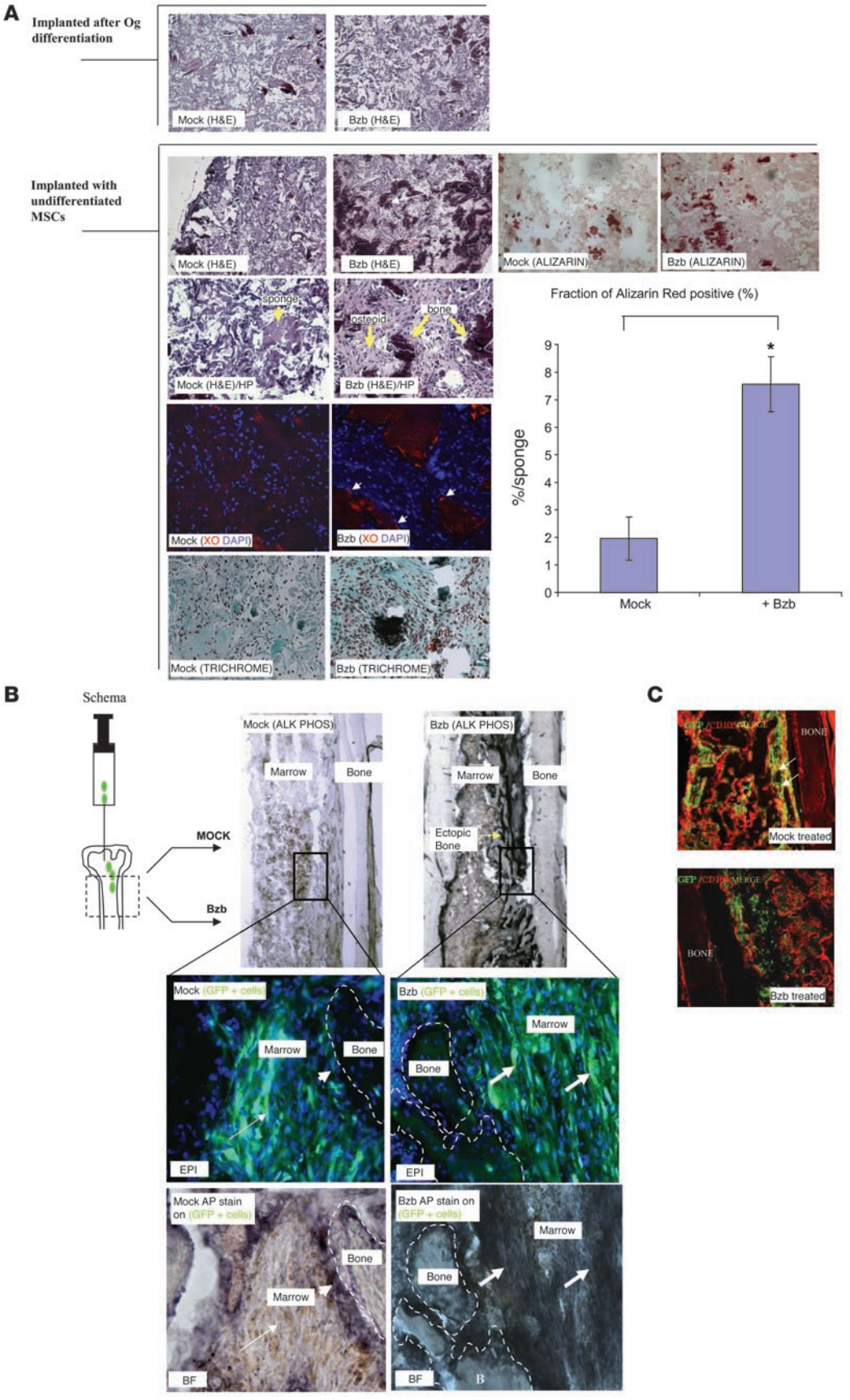
A
Implanted after Og differentiation
Mock (H&E)
Bzb (H&E)
Implanted with undifferentiated MSCs
Mock (H&E)
Bzb (H&E)
Mock (ALIZARIN)
Bzb (ALIZARIN)
sponge
osteoid
bone
Mock (H&E)/HP
Bzb (H&E)/HP
Mock (XO DAPI)
Bzb (XO DAPI)
Mock (TRICHROME)
Bzb (TRICHROME)
Fraction of Alizarin Red positive (%)
%/sponge
Mock
+ Bzb
B
Schema
MOCK
Bzb
Mock (ALK PHOS)
Bzb (ALK PHOS)
Marrow
Bone
Ectopic Bone
Mock (GFP + cells)
Bzb (GFP + cells)
EPI
Mock AP stain on (GFP + cells)
Bzb AP stain on (GFP + cells)
BF
C
BONE
Mock treated
Bzb treated

Figure 6
Bzb increases bone formation from MSCs in vivo. (**A**) Sponges embedded with cells differentiated in osteogenic medium (upper 2 panels) or loaded with undifferentiated MSCs (lower panels) were transplanted into immunocompromised mice, and recipient mice were treated with Bzb at 0.3 mg/kg i.p. for 10 doses. Bzb treatment had no observable impact on osteoblast-loaded sponges (upper 2 panels; stained with H&E). In MSC-loaded sponges (lower panels), osteoid and bone were increased upon Bzb treatment (yellow arrows), shown in low power (original magnification, ×40) or in high power (HP; original magnification, ×100). Bzb treatment also increased matrix-depositing cells, seen as cells (white arrows) adjacent to xylenol orange (XO) fluorescence (red) with DAPI nuclear counterstain. Increased bone upon Bzb treatment was also observed with trichrome stain and with alizarin red stain on control- and Bzb-treated sponges. Graph shows quantification of alizarin red–stained fraction of tissue in control- and Bzb-treated sponges. $^*P = 0.007$; $n = 3$. (**B**) Mice were implanted intrafemorally with GFP$^+$ MSCs and then treated with control or Bzb i.p. Upper panels show femurs containing implanted GFP$^+$ MSCs after treatment. Femurs were stained with alkaline phosphatase (purple). Increased ectopic bone is seen in Bzb-treated bones (arrows). Lower 4 panels show bright-field and epifluorescence images of the same section at higher magnification. Original magnification, ×20 (upper 2 panels); ×100 (lower 4 panels). In saline-treated animals, most GFP$^+$ cells remained Alkaline phosphatase negative (long arrow). Occasional GFP$^+$Alkaline phosphatase–positive cells were seen lining the endosteal surface (short arrows). In contrast, in Bzb-treated animals, increased ectopic bone was observed. Ectopic alkaline phosphatase–positive cells derived from GFP$^+$ MSCs (green) were frequently observed (lower 2 right panels, white arrows) not only next to the bone, but also in the marrow space. (**C**) In saline-treated animals, GFP$^+$ cells retained fibroblastoid appearance and CD105 positivity (GFP, green; CD105, red; double labeled, yellow; double-labeled cells are shown with white arrows in panel). In Bzb-treated animals, most cells lost their CD105 positivity (green). Images are from a single optical slice, using a confocal microscope. Original magnification, ×100.

For statistical analysis, the average dCt value (difference in amplification cycles required to detect the amplification product) and its standard deviation (sdCt) was used in a standard 2-tailed Student's *t* test.

Von Kossa assay and staining. CD105 cells isolated from MSC cultures (passage 2) were plated at 5000 cells/well in 96-well plates and differentiated in osteogenic medium as above at 33°C. At 8 days, cells were fixed and washed in water, and a 5% silver nitrate solution was added to the well under incandescent light for 20–45 minutes. After granules developed, the silver nitrate was removed and wells were washed with water to stop the reaction. Two images with a ×10 objective were obtained per well and the results quantified by ImageJ analysis.

In situ collagen I staining. For in situ collagen I staining, cells treated for 5 days with Bzb or DMSO were washed with PBS/0.5% FBS and exposed for 15 minutes to a rabbit anti-mouse collagen I antibody (21286; Abcam) diluted 1:200 in PBS. After incubation, the wells were washed 3 times and the secondary antibody, Alexa Fluor–conjugated anti-rabbit IgG, was added at 1:200. Wells were again washed 3 times and finally fixed with 2% PFA for 10 minutes prior to visualization by microscopy. Brightly positive collagen I clusters were quantified for each well.

Adipogenesis. For adipogenic differentiation, CD105$^+$ cells (passages 3–4) were plated at 1×10^4 cells/well in a 48-well plate (BD Biosciences) in an adipogenic induction medium: DMEM–low glucose (CellGro) with L-glutamine and penicillin and streptomycin solution (CellGro), 10% fetal bovine solution (HyClone), dexamethasone (50 μM), 3-isobutyl-1-methylxanthine (0.5 mM), insulin (10 μg/ml), and indomethacin (100 μM; Sigma-Aldrich) at 33°C. After 4 days of induction, cells were switched to DMEM with 10% FCS containing 5 μM rosiglitazone and insulin (10 μg/ml) and dexamethasone (50 μM), again maintaining Bzb concentration indicated. Oil red O staining was carried out on day 5 per the manufacturer's instructions (Electron Microscopy Sciences).

Implantation of MSCs in collagen sponges. Three-dimensional collagen scaffolds (BD Biosciences) were soaked overnight in α20%. Cultured hMSCs were resuspended at 2×10^6 in 30 μl PBS and pipetted directly on top of each scaffold and cultured for 7 days in MSC basal medium to generate MSC-implanted sponges. Another set of sponges was switched to osteogenic medium 1 day after implantation of cells and cultured for 7 additional days (osteoblast-implanted sponges). Beige nude XID mice (female, 6–7 weeks; Harlan Sprague) were anesthetized, and a small pocket was formed subcutaneously. A single scaffold was gently inserted into the pocket (30). The mice were then treated with Bzb or control saline, as described above, for 10 doses (3 doses/week, given on alternate days — Mondays, Wednesdays and Fridays — at 0.3 mg/kg i.p.).

Direct intrafemoral injection of MSCs. C57BL/6 mice (Jackson Laboratories) were anesthetized, and a small incision was made over the right knee to gain access to the kneecap. A 27-gauge needle was used to drill a hole in the femur, and 20 μl of cultured GFP-positive MSCs at 5×10^7 cells/ml was slowly injected into the cavity with a 26-gauge Hamilton Microliter Syringe (31). The mice were then treated with Bzb or control saline, as described above, for 6 doses (3 doses/week, given on alternate days — Mondays, Wednesdays and Fridays — at 0.3 mg/kg i.p.).

Isolation of Ops from Osx-GFP mice. Femurs and spine from 6-week-old *Osx-GFP* mice were isolated and crushed with mortar and pestle. Supernatant was pooled and kept aside (to generate the first fraction). The bone fragments were digested with collagenase I at 37°C and 1 hour in a shaking water bath. Collagenase was inactivated with excess PBS containing 1% FCS and washing with medium containing 20% serum. The bone slurry was then triturated extensively to dislodge all remaining cells and filtered through a 70-μm filter; the material was pooled with cells from the first fraction. The cells were then treated as described for crushed bone marrow samples.

Osteoclast differentiation. Bone marrow from 8-week-old C57BL/6 mice was harvested. 1×10^5 mononuclear cells/well were plated in flat-bottom 96-well plates in α-MEM (CellGro) containing 10% FCS (HyClone). Osteoclastogenesis was induced by adding M-CSF (20 ng/ml, R+D) and RANKL (200 ng/ml, gift of Yongwon Choi, The Leonard and Marilyn Abramson Family Cancer Research Institute, University of Pennsylvania, Philadelphia, Pennsylvania, USA) in the presence of 1 nM or 2 nM Bzb. After 5 days, culture supernatants were analyzed for TRAP activity and cells were fixed and stained for TRAP cytochemistry (Sigma-Aldrich).

Immunoblotting for Runx-2. Primary MSCs cultured with Bzb (10 nM) or lactacystin (20 μM) for 6 hours were harvested, washed, and lysed using RIPA buffer: 50 mM Tris-HCl (pH 7.4), 150 mM NaCl, 1% NP-40, 0.5% sodium deoxycholate, 5 mM EDTA, 5 mM NaF, 1 mM Na_3VO_4, 1 mM PMSF, 5 μg/ml leupeptine, and 5 μg/ml aprotinin. Whole-cell lysates were subjected to SDS-PAGE, transferred to a PVDF membrane (Bio-Rad Laboratories), and immunoblotted with anti–Runx-2 (Calbiochem) and GAPDH (Santa Cruz Biotechnology Inc.) antibodies.

Micro-CT analysis of femurs. Micro-CT analysis was carried out as described in Pierroz et al. (41). In brief, femurs were dissected, cleaned, fixed in 4% paraformaldehyde, loaded onto CT scanning devices, and imaged according to the protocol previously described (41).

hMSC culture. For in vitro osteoblast and adipocyte differentiation, hMSCs (Cambrex) were maintained and differentiated following the manufacturer's protocol. Cambrex cells are typically obtained at passage 3. For the quantita-

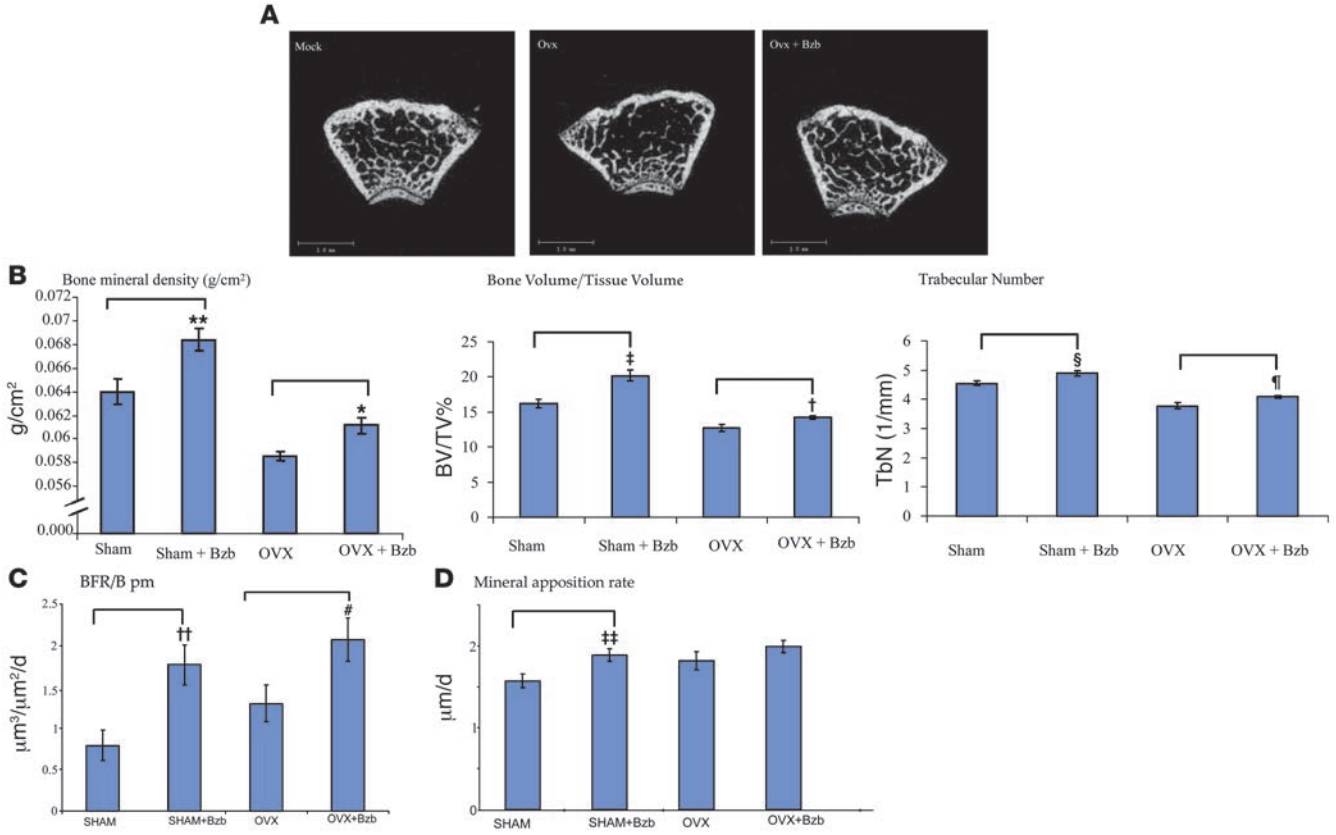

Figure 7

Bzb rescues osteoporosis in ovariectomized mice. FVB/N female mice were ovariectomized at week 9 and treated with saline or 0.3 mg/kg Bzb for 6 weeks (18 doses) starting at week 11.5. (**A**) Representative micro-CT analysis of cross sections of trabecular bone are shown for mock-treated, ovariectomized, and ovariectomized/Bzb-treated mice. Scale bar: 1.0 mm. (**B**) Baseline distal femur BMD increased upon Bzb treatment in both mock-treated and ovariectomized mice. $^{*}P = 0.006$; $^{**}P = 0.03$; $n = 10$ femurs/group. Quantitative analysis by micro-CT scanning revealed that ovariectomized animals had decreases in trabecular bone volume fraction and that Bzb treatment partly rescued this decrease. $^{\ddagger}P = 0.001$; $^{\dagger}P = 0.01$; $n = 10$ femurs/group. Trabecular number/mm decreased with ovariectomy but was rescued by Bzb treatment. $^{\P}P = 0.01$; $^{\S}P = 0.002$; $n = 10$ femurs/group. (**C**) BFR per BSpm (BFR/B pm) was increased in ovary-intact animals by Bzb treatment ($^{\#}P = 0.007$; $n = 7$ femurs) and also increased in ovariectomized animals ($^{\dagger\dagger}P = 0.05$; $n = 7$ femurs). (**D**) Mineral apposition rate was increased in ovary-intact animals ($^{\ddagger\ddagger}P = 0.01$; $n = 7$ femurs) with Bzb treatment. In ovariectomized animals, there was increased mineral apposition, but the effect was not significant. $P = 0.1$.

tive alkaline phosphatase assay and osteoblast differentiation, hMSCs (passages 4–5) were plated in Optilux 96-well plates (BD Biosciences) at a concentration of 3.1×10^3 cells/cm² in MSC growth medium (MSGM). Following an overnight incubation, the growth medium was replaced with osteogenic induction medium that contained Bzb or vehicle. Cells were cultured in the presence of Bzb or vehicle for 6 days, at which point osteoblast differentiation was assayed by alkaline phosphatase expression (described below). For adipogenesis, hMSCs were plated in MSGM at a concentration of 2×10^5 cells/well of a 6-well plate. MSCs were maintained in MSGM until the cells reached confluency. Cells were then cultured for 3 days in adipogenic induction medium (Chemicon) in the presence of Bzb or vehicle. The cells were then cultured for 1 day in adipogenic maintenance medium per manufacturer's protocol (Chemicon) followed by another 3-day culture period in adipogenic induction medium. At each medium change, Bzb or vehicle was added fresh to the cultures. Following the last culture period in adipogenic induction medium, adipogenesis was assessed by fixing cells with 10% neutral-buffered formalin (VWR) and staining with oil red O to visualize lipid droplets.

Luciferase reporter assay for osteocalcin. C3H10T1/2 cells (ATCC) were grown in DMEM with 10% FCS. Cells were plated into 12-well plates at 60,000 cells/well. One day after plating, cells were transfected with the indicated combinations of 6xOSE2-*luciferase*, pTK-RL, and *Runx-2* expression constructs using Effectene transfection reagent (QIAGEN). 18 hours later, the medium was changed and the indicated concentration of Bzb was added. 24 hours later, cells were harvested and firefly/renilla luciferase activity was determined per the manufacturer's instructions (Promega). Each experiment was performed in triplicate and repeated at least 3 times. 6xOSE2-luciferase and Runx-2 expression constructs and additional methods are described in ref. 27.

qPCR analysis of mouse embryonic cells. Mouse embryonic mesodermal fibroblasts were isolated 12.5 dpc from WT and *Runx-2*$^{-/-}$ mice as previously described (42). In brief, individual embryos were homogenized using an 18-gauge syringe in the presence of 0.25% trypsin and 1 mM EDTA (Invitrogen). The trypsin was inactivated after 15 minutes by addition of DMEM supplemented with 15% fetal bovine serum (Hyclone), 2 mM L-glutamine, 20 U/ml penicillin, and 20 µg/ml streptomycin. Cells were plated and allowed to adhere for 24 hours. For these experiments, WT and *Runx-2*$^{-/-}$ cells were replated in 6-well plates at densities of 8×10^4 and 5×10^4 cells/well, respectively. Because *Runx-2*$^{-/-}$ osteoblasts proliferate more quickly than WT osteoblasts, these seeding densities allowed cells to reach confluency at the same time (39). After overnight adher-

ence, cells were treated with 1.5 nM Bzb. DMSO (1.5 μl/ml) was used for control cells. When cells were near confluency (day 4), the medium was replaced with an osteogenic medium (αMEM supplemented with 15% FBS [SH30070.03; HyClone], 2 mM L-glutamine, 20 U/ml penicillin, 20 μg/ml streptomycin, 25 μg/ml ascorbic acid, and 10 mM β-glycerophosphate). Cells were harvested 5 days after plating, and RNA was isolated using TRIZOL (Invitrogen) according to the manufacturer's protocol. Oligo-dT primers were used in conjunction with the SuperScript First-Strand Synthesis System (Invitrogen) to synthesize cDNAs. mRNA levels of osteoblast-related genes were analyzed by real-time qPCR using the Power SYBR Green Master Mix (Applied Biosystems) on an ABI PRISM 7000 sequence detection system (Applied Biosystems). Primer sequences are as follows: *Alp*: forward, TTGTGCGAGAGAAAGAGAGAGA, reverse, GTTTCAGGGCATTTTTCAAGGT; *BSP*: forward, GCACTCCAACTGCCCAAGA, reverse, TTTTGGAGCCCTGCTTTCTG; *Col1a1*: forward, CCCAAGGAAAAGAAGCACGTC, reverse, AGGTCAGCTGGATAGCGACATC; *mCox*: forward, ACGAAATCAACAACCCCGTA, reverse, GGCAGAACGACTCGGTTATC; and *Runx-2*: forward, CGGCCCTCCCTGAACTCT, reverse, TGCCTGCCTGGGATCTGTA. Transcript levels were normalized to mitochondrial cytochrome *c* oxidase subunit II (mCox) or *GAPDH* and are expressed relative to WT control cells.

API. To determine the API, cell numbers were first established by culturing cells in medium containing Alamar Blue (Biosource) for 4 hours at 37°C. Plates were read on a fluorimeter at 570 nm. Medium containing Alamar Blue was removed, and cells were washed once with sterile PBS. Cells were then incubated with alkaline phosphatase substrate (Sigma-Aldrich) for 1 hour at room temperature. The plate was read at 405 nm. Alkaline phosphatase levels were then normalized to cell number to establish API (API = alkaline phosphatase fluorimeter reading/Alamar Blue fluorimeter reading × 1000).

Ovariectomy and Bzb treatment. Nine-week-old FVB/N female mice were ovariectomized by a commercial vendor (Charles River Laboratories). Bzb treatment was initiated an additional 2.5 weeks later and given i.p. at 0.3 mg/kg Mondays, Wednesdays, and Fridays for a total of 6 weeks.

Osteoclast resorption assays. Osteoclast resorption was carried out as described (43). Resorption pits were stained and imaged with a ×20 objective and average pit size calculated by ImageJ analysis of the stained sections.

Statistics. In all cases, analysis was performed by a standard 2-tailed Student's *t* test. The maximum number of independently compared variables was limited to 2 for any experiment. All data have been plotted as average ± SEM.

Acknowledgments

This work is supported by NIH grants P01 CA082834 (to G. Stein); HL081030, HL044851, and DK050234 (to D.T. Scadden); and K08 HL085872 (to S. Mukherjee).

Received for publication June 26, 2007, and accepted in revised form November 28, 2007.

Address correspondence to: David T. Scadden, Center for Regenerative Medicine, Massachusetts General Hospital, 185 Cambridge Street, Boston, Massachusetts 02115, USA. Phone: (617) 726-5615; Fax: (617) 724-2662; E-mail: dscadden@mgh.harvard.edu.

1. Friedenstein, A.J., Piatetzky, S., II, and Petrakova, K.V. 1966. Osteogenesis in transplants of bone marrow cells. *J. Embryol. Exp. Morphol.* **16**:381–390.
2. Friedenstein, A.J., Chailakhyan, R.K., Latsinik, N.V., Panasyuk, A.F., and Keiliss-Borok, I.V. 1974. Stromal cells responsible for transferring the microenvironment of the hemopoietic tissues. Cloning in vitro and retransplantation in vivo. *Transplantation.* **17**:331–340.
3. Horwitz, E.M., et al. 1999. Transplantability and therapeutic effects of bone marrow–derived mesenchymal cells in children with osteogenesis imperfecta. *Nat. Med.* **5**:309–313.
4. Prockop, D.J. 1997. Marrow stromal cells as stem cells for nonhematopoietic tissues. *Science.* **276**:71–74.
5. Mangi, A.A., et al. 2003. Mesenchymal stem cells modified with Akt prevent remodeling and restore performance of infarcted hearts. *Nat. Med.* **9**:1195–1201.
6. Ding, S., and Schultz, P. 2005. Small molecules and future regenerative medicine. *Curr. Top. Med. Chem.* **5**:383–395.
7. Shimazaki, C., et al. 2005. High serum bone-specific alkaline phosphatase level after bortezomib-combined therapy in refractory multiple myeloma: possible role of bortezomib on osteoblast differentiation. *Leukemia.* **19**:1102–1103.
8. Zangari, M., et al. 2005. Response to bortezomib is associated to osteoblastic activation in patients with multiple myeloma. *Br. J. Haematol.* **131**:71–73.
9. Shen, R., et al. 2006. Smad6 interacts with Runx–2 and mediates Smad ubiquitin regulatory factor 1–induced Runx–2 degradation. *J. Biol. Chem.* **281**:3569–3576.
10. Garrett, I.R., et al. 2003. Selective inhibitors of the osteoblast proteasome stimulate bone formation in vivo and in vitro. *J. Clin. Invest.* **111**:1771–1782.
11. Giuliani, N., et al. 2007. The proteasome inhibitor bortezomib affects osteoblast differentiation in vitro and in vivo in multiple myeloma patients. *Blood.* **110**:334–338.
12. Meirelles Lda, S., and Nardi, N.B. 2003. Murine marrow-derived mesenchymal stem cell: isolation, in vitro expansion, and characterization. *Br. J. Haematol.* **123**:702–711.
13. Sun, S., et al. 2003. Isolation of mouse marrow mesenchymal progenitors by a novel and reliable method. *Stem Cells.* **21**:527–535.
14. Anjos-Afonso, F., Siapati, E.K., and Bonnet, D. 2004. In vivo contribution of murine mesenchymal stem cells into multiple cell-types under minimal damage conditions. *J. Cell Sci.* **117**:5655–5664.
15. Quarto, N., and Longaker, M.T. 2006. FGF-2 inhibits osteogenesis in mouse adipose tissue-derived stromal cells and sustains their proliferative and osteogenic potential state. *Tissue Eng.* **12**:1405–1418.
16. Nakashima, K., et al. 2002. The novel zinc finger-containing transcription factor osterix is required for osteoblast differentiation and bone formation. *Cell.* **108**:17–29.
17. Rodda, S.J., and McMahon, A.P. 2006. Distinct roles for Hedgehog and canonical Wnt signaling in specification, differentiation and maintenance of osteoblast progenitors. *Development.* **133**:3231–3244.
18. Jaiswal, N., Haynesworth, S.E., Caplan, A.I., and Bruder, S.P. 1997. Osteogenic differentiation of purified, culture-expanded human mesenchymal stem cells in vitro. *J. Cell Biochem.* **64**:295–312.
19. Janderova, L., McNeil, M., Murrell, A.N., Mynatt, R.L., and Smith, S.R. 2003. Human mesenchymal stem cells as an in vitro model for human adipogenesis. *Obes. Res.* **11**:65–74.
20. Pittenger, M.F., et al. 1999. Multilineage potential of adult human mesenchymal stem cells. *Science.* **284**:143–147.
21. Dominici, M., et al. 2006. Minimal criteria for defining multipotent mesenchymal stromal cells. The International Society for Cellular Therapy position statement. *Cytotherapy.* **8**:315–317.
22. Mundlos, S., et al. 1997. Mutations involving the transcription factor CBFA1 cause cleidocranial dysplasia. *Cell.* **89**:773–779.
23. Otto, F., et al. 1997. Cbfa1, a candidate gene for cleidocranial dysplasia syndrome, is essential for osteoblast differentiation and bone development. *Cell.* **89**:765–771.
24. Tintut, Y., Parhami, F., Le, V., Karsenty, G., and Demer, L.L. 1999. Inhibition of osteoblast-specific transcription factor Cbfa1 by the cAMP pathway in osteoblastic cells. Ubiquitin/proteasome-dependent regulation. *J. Biol. Chem.* **274**:28875–28879.
25. Gori, F., Thomas, T., Hicok, K.C., Spelsberg, T.C., and Riggs, B.L. 1999. Differentiation of human marrow stromal precursor cells: bone morphogenetic protein-2 increases OSF2/CBFA1, enhances osteoblast commitment, and inhibits late adipocyte maturation. *J. Bone Miner. Res.* **14**:1522–1535.
26. Banerjee, C., et al. 2001. Differential regulation of the two principal Runx-2/Cbfa1 n-terminal isoforms in response to bone morphogenetic protein-2 during development of the osteoblast phenotype. *Endocrinology.* **142**:4026–4039.
27. Jones, D.C., et al. 2006. Regulation of adult bone mass by the zinc finger adapter protein Schnurri-3. *Science.* **312**:1223–1227.
28. Komori, T., et al. 1997. Targeted disruption of Cbfa1 results in a complete lack of bone formation owing to maturational arrest of osteoblasts. *Cell.* **89**:755–764.
29. Lengner, C.J., et al. 2005. Nkx3.2-mediated repression of Runx-2 promotes chondrogenic differentiation. *J. Biol. Chem.* **280**:15872–15979.
30. Kuznetsov, S.A., et al. 2004. The interplay of osteogenesis and hematopoiesis: expression of a constitutively active PTH/PTHrP receptor in osteogenic cells perturbs the establishment of hematopoiesis in bone and of skeletal stem cells in the bone marrow. *J. Cell Biol.* **167**:1113–1122.
31. Wang, L., Liu, Y., Kalajzic, Z., Jiang, X., and Rowe, D.W. 2005. Heterogeneity of engrafted bone-lining cells after systemic and local transplantation. *Blood.* **106**:3650–3657.
32. Elsubeihi, E.S., Bellows, C.G., Jia, Y., and Heersche, J.N. 2007. Ovariectomy of 12-month-old

rats: effects on osteoprogenitor numbers in bone cell populations isolated from femur and on histomorphometric parameters of bone turnover in corresponding tibia. *Cell Tissue Res.* **330**:515–526.
33. Sheng, M.H., et al. 1999. Histomorphometric studies show that bone formation and bone mineral apposition rates are greater in C3H/HeJ (high-density) than C57BL/6J (low-density) mice during growth. *Bone.* **25**:421–429.
34. Barnes, G.L., et al. 2003. Osteoblast-related transcription factors Runx-2 (Cbfa1/AML3) and MSX2 mediate the expression of bone sialoprotein in human metastatic breast cancer cells. *Cancer Res.* **63**:2631–2637.
35. Delmas, P.D. 2002. Treatment of postmenopausal osteoporosis. *Lancet.* **359**:2018–2026.
36. Bilezikian, J.P. 2006. Osteonecrosis of the jaw — do bisphosphonates pose a risk? *N. Engl. J. Med.* **355**:2278–2281.
37. Tian, E., et al. 2003. The role of the Wnt–signaling antagonist DKK1 in the development of osteolytic lesions in multiple myeloma. *N. Engl. J. Med.* **349**:2483–2494.
38. Yaccoby, S., et al. 2006. Antibody-based inhibition of DKK1 suppresses tumor-induced bone resorption and multiple myeloma growth in vivo. *Blood.* **109**:2106–2111.
39. Hideshima, T., et al. 2001. The proteasome inhibitor PS-341 inhibits growth, induces apoptosis, and overcomes drug resistance in human multiple myeloma cells. *Cancer Res.* **61**:3071–3076.
40. Zarrinkalam, K.H., Kuliwaba, J.S., Martin, R.B., Wallwork, M.A., and Fazzalari, N.L. 2005. New insights into the propagation of fatigue damage in cortical bone using confocal microscopy and chelating fluorochromes. *Eur. J. Morphol.* **42**:81–90.
41. Pierroz, D.D., Bouxsein, M.L., Rizzoli, R., and Ferrari, S.L. 2006. Combined treatment with a beta–blocker and intermittent PTH improves bone mass and microarchitecture in ovariectomized mice. *Bone.* **39**:260–267.
42. Pratap, J., et al. 2003. Cell growth regulatory role of Runx–2 during proliferative expansion of preosteoblasts. *Cancer Res.* **63**:5357–5362.
43. Vallet, S., et al. 2007. MLN3897, a novel CCR1 inhibitor, impairs osteoclastogenesisand inhibits the interaction of multiple myeloma cells and osteoclasts. *Blood.* **110**:3744–3752.